Desalination and Water Treatment
www.deswater.com

doi:10.5004/dwt.2017.21017

82 (2017) 262–270
July

Kinetics and adsorption isotherm for the removal of fluoride and chromium (VI) from wastewater by electrocoagulation

S. Aoudj[a,d], B. Cheknane[b], H. Zemmouri[c], F. Zermane[b], A. Khelifa[d], M. Hecini[a,d], N. Drouiche[a,*]

[a]*CRTSE-Division CCPM- N°2, Bd Dr. Frantz FANON- p.o.box 140, Alger sept merveilles, 16038, Algeria, email: salahaoudj@yahoo.com (S. Aoudj), mounasfn@yahoo.fr (M. Hecini), Tel. +213 21 279880 Ext 172, Fax +213 21 433511, email: nadjibdrouiche@yahoo.fr (N. Drouiche)*
[b]*Laboratoire Eau Environnement et Développement Durable, Faculté de Technologie, Université Blida 1, BP 270, 09000 Blida, Algeria, email: ocheknane@yahoo.fr (B. Cheknane), zermanefaiza@yahoo.fr (F. Zermane)*
[c]*Faculté de Génie Mécanique et Génie des Procédés, Université des Sciences et de la Technologie Houari Boumediene, Algiers, Algeria, email: hassiba_zemmouri@yahoo.fr (H. Zemmouri)*
[d]*Laboratoire de génie chimique, Département de Chimie Industrielle, Université Saad Dahlab, B.P. 270, Route de Soumaa 09000, Blida, Algeria, email: khelifaab@hotmail.com (A. Khelifa)*

Received 16 January 2017; Accepted 6 June 2017

ABSTRACT

In this work, the removal of fluoride and Cr(VI) by electrogenerated coagulants is studied in single and binary systems. The effects of initial pH, current intensity and initial concentration on fluoride and hexavalent chromium removal were investigated. The results showed that an optimum removal was achieved at an initial pH of 3.0. Removal efficiencies of 96.7% and 97.4% were achieved for fluoride and Cr(VI) respectively at that pH. Adsorption kinetics showed that the first order rate expression fitted the adsorption kinetics for both fluoride and Cr(VI). The equilibrium isotherm was analyzed by Langmuir and Freundlich isotherm models. The characteristic parameters for each isotherm were determined. The Freundlich adsorption isotherm was found to fit well the equilibrium data for both fluoride and Cr(VI) adsorptions. Kinetics of adsorption of the two pollutants onto aluminium hydroxides in binary system at different ratios (r = [Cr]/[F^-]) showed that the presence of one of the pollutants can influence strongly the absorption of other which confirms the antagonistic effect during the adsorption. The temperature studies showed that adsorption was endothermic and spontaneous nature for both pollutants.

Keywords: Fluoride; Chromium (VI); Electrocoagulation; Kinetics; Adsorption isotherm modeling; Competition

1. Introduction

The fabrication of silicon solar cells requires huge amounts of chemicals and large volumes of ultra-pure water and therefore generates large volumes of wastewaters [1,40–43]. Many toxic contaminants are currently found in this type of wastewater including acids, heavy metals, solvents, surfactants, complexing agents, salts, suspended particles, etc. The acidic waste is the dominant class and the more environment threatening of this wastewater [2]. Waste sulfuric, hydrofluoric, hydrochloric, nitric, and chromic acids are produced as a result of silicon wafer surface etching. In the case of Secco and Yang etching processes [3–5] formulations with hydrofluoric/chromic acids are currently used. Thus, both toxic ions of fluoride and Cr(VI) are found in the photovoltaic industry effluents in concentration levels much higher than allowed values [6]. Currently, lime precipitation associated with coagulation is used as effluent treatment. This process, however, suffers from some drawbacks like high addition of chemicals and generation of large volume of sludge [7,8].

*Corresponding author.

In recent years, several innovative technologies were developed for the removal of many pollutants [9,10]. Electrochemical methods know an increasing interest to remedy deficiencies of existing chemical processes [11–13]. Electrocoagulation (EC) has been successfully used as an alternative method. Compared with chemical coagulation, it proved to be more effective in removing inorganic contaminants. EC is a potentially effective method for treating different kinds of wastewater with high removal efficiency [14,44].

EC consists of *in situ* electrogeneration of coagulants Al^{3+} or Fe^{2+} by means of electrodissolution of aluminum and iron anodes respectively [15]. In the case of aluminum, the main reactions are given as follows:

$$\text{Anode: } Al \rightarrow Al^{3+} + 3e^{-} \quad (1)$$

$$\text{Cathode: } 2H_2O + 2e\text{-} \rightarrow 2OH^{-} + H_2 \quad (2)$$

$$Al^{3+} + 3H_2O \rightarrow Al(OH)_{3(s)} + 3H^{+} \quad (3)$$

The formed $Al(OH)_{3(s)}$ flocs have large surface areas, and hence may be excellent adsorbents for soluble compounds. These flocs are removed easily from treated solutions by sedimentation or flotation.

In spite of the extensive literature about the application of EC on water and wastewater treatment, more investigation needs to be done in order to deepen the knowledge concerning the removal mechanisms. In addition, most studies focused in the study of optimization of influencing parameters; there is still a lack in modeling this process and investigation of involved phenomena. In this context, some studies [16–24] were recently done for exploring kinetics and isotherm adsorption modeling in this case of EC treatment. This is because the electrochemically generated coagulants act as adsorbent for pollutant removal.

In this paper, the EC process using aluminium anode was used to treat synthetic solutions containing fluoride and Cr(VI) ions. The treatment of the pollutants was first carried out separately and then simultaneously. The effect of parameters such as initial pH, current intensity, initial concentration and temperature was done. Consequently, adsorption kinetics of electrocoagulants is analyzed using first- and second-order kinetic models. The equilibrium adsorption behavior is analyzed by fitting the isotherm models of Langmuir and Freundlich. Activation energy was evaluated to study the nature of adsorption.

2. Experimental

2.1. Experimental setup

2.1.1. Electrocoagulation cell

The EC unit consists of an electrochemical reactor which is a glass beaker with magnetic stirring, a D.C. power supply (Metrix AX502, 0–2.5 A and 0–30 V) and two electrodes. The cathode was of stainless steel and anode was of aluminium, each one with dimensions of (5 cm × 17 cm × 0.2 cm). The submerged surface area of the each electrode plate was 40 cm^2. The gap between the electrodes was 1.5 cm. An ammeter (Chauvin-Arnoux C.A 401) and voltmeter (DIGITAL VOLTMETER (G-1002-500)) were used to check the current and the voltage during EC process. The temperature of the solution was controlled at a desired value by thermostatically controlled water.

2.2. Experimental procedure

In order to simulate semiconductor wastewater desired amounts of NaF and $K_2Cr_2O_7$ are added to the solution. Samples were periodically withdrawn and they were immediately filtered through 0.22 µm nylon syringe filter in order to measure fluoride and Cr(VI) concentrations. For the characterization purpose, generated sludge was filtered and washed then dried at 105°C for 24 h.

2.3. Analytical methods

Combined selective ion electrode (HI 4222 HANNA with a HI 4110 probe) was used to determine the fluoride concentration according to the ionometric standard method [25]. Concentration of Cr(VI) was measured using the 1–5 diphenylcarbazide method [25] with a HACH DR 2500 spectrophotometer. The pH values were determined by using pH meter (HI 4222 HANNA with a HI 1131 probe).

2.4. Characterization techniques

FT-IR analysis was carried out by JASCO FT/IR-4100 spectrometer and the results were obtained with OMNIC software.

3. Results and discussion

3.1 Effect of initial pH

Initial pH is a determining factor in the electrochemical process [14,17]. Solution pH affects both adsorbent surface characteristics and pollutants species. Initial pH effect was studied from 3 to 9 to determine its effect on removal efficiencies of fluoride and Cr(VI) removal. The results are shown in Figs. 1 and 2 respectively. From Fig. 1 it can be observed that initial pH has significant effect on fluoride

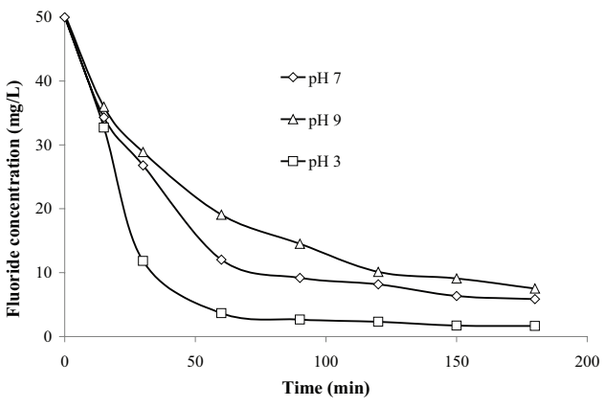

Fig. 1. Effect of initial pH on fluoride removal, $[F^-]_0$, 50 mg/L; current intensity 400 mA.

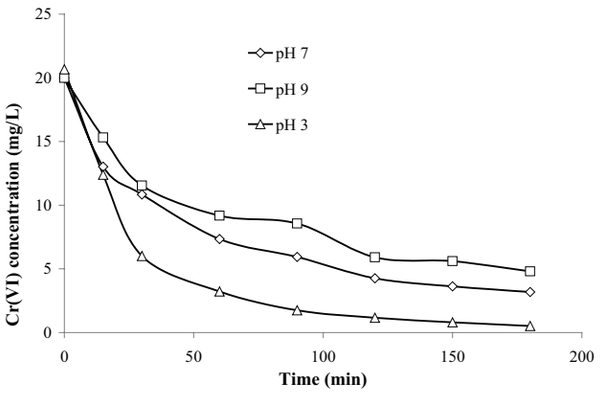

Fig. 2. Effect of initial pH on Cr(VI) removal, $[Cr(VI)]_0$, 20 mg/L; current intensity 400 mA.

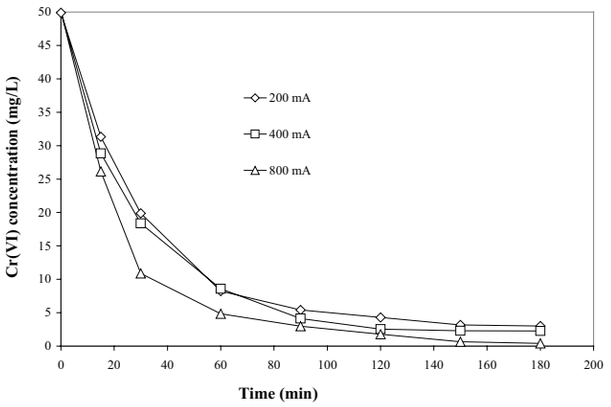

Fig. 3. Effect of current intensity on Cr(VI) removal, pH_0, 3; $[Cr(VI)]_0$, 50 mg/L.

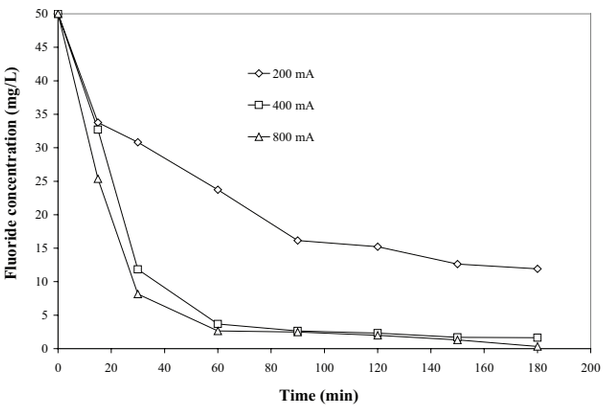

Fig. 4. Effect of current intensity on fluoride removal, pH_0, 3; $[F^-]_0$, 50 mg/L.

removal. Decrease of initial pH results in lower fluoride concentration. At 180 min, when the initial pH values are 3, 7 and 9 final fluoride concentrations are 1.63, 5.86, and 7.50 mg/L respectively. Similar result was observed by Hu et al. [7] who found that an initial pH of about 3 gives optimal fluoride efficiencies. At the acidic pH, aluminum cations produced at the anode formed polymeric species and precipitated $Al(OH)_3$ leading to better removal efficiency [26]. Decreasing in removal efficiency at alkaline pH was attributed to the formation of soluble $Al(OH)_4^-$ anions in detriment of $Al(OH)_3$. From Fig. 2 it can be observed that initial pH has strong effect on Cr(VI) removal. The Cr(VI) removal rate and extent increase when initial pH decreases. Acidic media are suitable for Cr(VI) removal, while the abetment slowed down at the alkaline media. While residual Cr(VI) concentration was 4.8 mg/L at initial pH 9 after 180 min treatment. The lowest Cr(VI) final concentration was observed at pH 3 with 0.52 mg/L. Similar results were found by Sadeghi et al. [26] who found that the highest Cr(VI) removal efficiency of about 78.8% was observed at pH 3 when studying hexavalent chromium removal by EC-Al. Hexavalent chromium may exist as H_2CrO_4, $HCrO_4^-$, $Cr_2O_7^{2-}$ and CrO_4^{2-} depending on solution pH and Cr(VI) concentration. At Cr(VI) concentrations less than 520 mg/L, CrO_4^{2-} is the predominant species above pH 6.5 and $HCrO_4^-$ predominates in pH range of 0.9–6.5 [27]. The aluminum hydroxide precipitate is known to be positively charged at lower pH values [28]. The negatively charged CrO_4^{2-} and/or $HCrO_4^-$ anions should adsorb on the positively charged aluminum hydroxide precipitates. Under alkaline conditions the formation of negatively charged aluminum hydroxide precipitate is not suitable for CrO_4^{2-} adsorption [27].

3.2 Effect of current intensity

Current densities ranging from 200 to 800 mA were used to investigate the effect of current intensity on EC efficiency. As shown in Fig. 3, increasing current intensity results in improvement of fluoride removal. Final concentration of 11.93 mg/L was obtained with 200 mA, while 800 mA lead to a residual concentration of 0.34 mg/L after 180 min. The impact of current intensity on the Cr(VI) removal efficiency is shown in Fig. 4. With an increase of current intensity, the removal of Cr(VI) was favorable. After 180 min of treatment, a concentration of 3.01 mg/L was found under a current of 200 mA. However, the residual concentration dropped to 0.4 mg/l under a current of 800 mA. Identical result was found by Vasudevan et al. [17] who achieved a series of experiments using 5 mg L^{-1} chromium-containing electrolyte, at pH 7.0, removal efficiencies of chromium are 96.2 and 99.6% when current densities are 0.1–0.5 A dm^{-2} respectively. This may be explained by the production of more aluminium adsorbing species generated by anode electrodissolution. Consequently, the amount of fluoride and hexavalent chromium adsorption increases with the increase in adsorbent concentration, indicating that the adsorption depends upon the availability of binding sites for both pollutants.

3.3 Effect of initial concentration

The study the effect of initial concentration was conducted by varying initial concentrations in the range of 20–150 mg/L. Results are depicted in Figs. 5 and 6. The final concentrations were 26.21 and 0.3 mg/l for initial fluoride concentrations of 150 and 25 mg/L, respectively; while

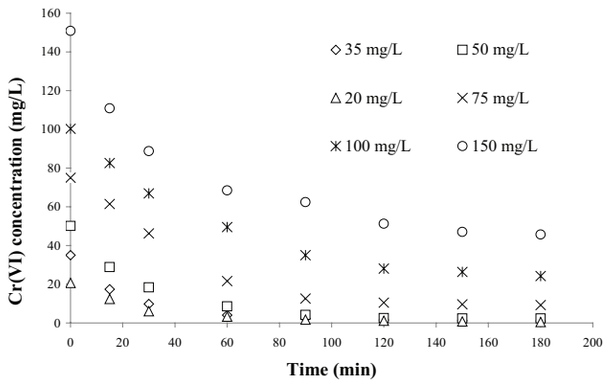

Fig. 5. Effect of initial concentration on Cr(VI) removal, pH_0, 3; current intensity 400 mA.

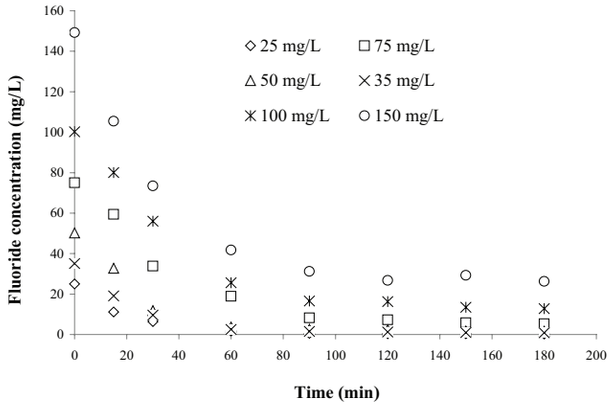

Fig. 6. Effect of initial concentration on fluoride removal, pH_0, 3; current intensity 400 mA.

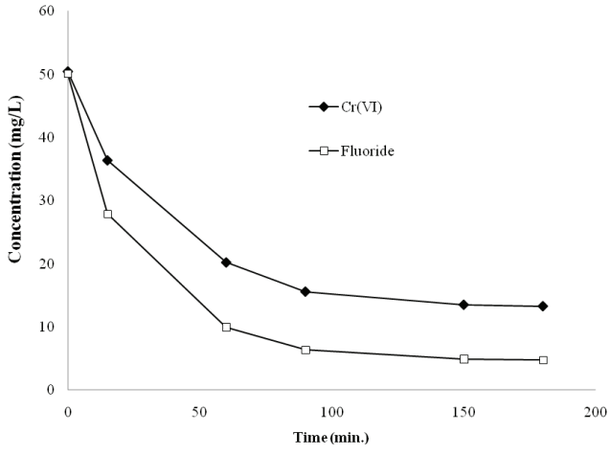

Fig. 7. Variation of fluoride and Cr(VI) concentrations in function of time. pH_0, 3; current intensity 400 mA; $[F^-]_0$, 50 mg/L; $[Cr(VI)]_0$, 50 mg/L.

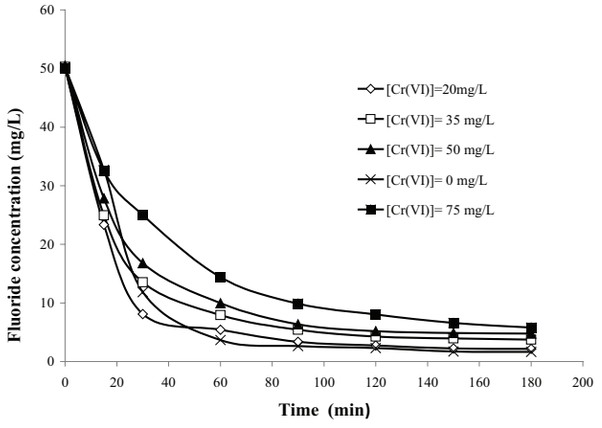

Fig. 8. Effect of Cr(VI) concentration on fluoride removal, pH_0, 3; current intensity 400 mA; $[F^-]_0$, 50 mg/L.

the final Cr(VI) concentrations were 45.69 and 0.52 mg/l for initial concentrations of 150 and 20 mg/L, respectively. Therefore, the pollutant removal efficiency is reduced by increasing the initial corresponding concentrations [26].

3.4. Competition effect

Fig. 7 represents the variation of fluoride and Cr(VI) concentrations in function of time at initial pH 3, current intensity 400 mA and using fluoride of 50 mg/l and Cr(VI) of 50 mg/l. This result mainly showed that $Al(OH)_3$ adsorbent is efficient for simultaneous removal of fluoride and Cr(VI) anions. The removal of fluoride in absence and presence of Cr(VI) anions was studied. Different initial Cr(VI) concentrations ranging from 20 to 75 mg/L were used. The results are depicted in Fig. 8. The removal efficiency is highest in absence of Cr(VI) anions. The final fluoride concentration increases with increasing Cr(VI) initial concentration. Final concentration of 1.65 mg/L was obtained in absence of Cr(VI), while in presence of Cr(VI) initial concentration of 75 mg/L leads to a residual fluoride concentration of 5.78 mg/L after 180 min. The presence Cr(VI) ions significantly inhibits the fluoride removal suggesting competing effect between fluoride and Cr(VI) anions. Similarly, Cr(VI) removal in absence and presence of fluoride anions was studied. Different initial fluoride concentrations ranging from 20 to 75 mg/L were used. The results are illustrated in Fig. 9. The lowest residual Cr(VI) concentrations are obtained in absence of fluoride ions with final concentration of 2.26 mg/L while in presence of fluoride initial concentration of 75 mg/L leads to a residual Cr(VI) concentration of 16.12 mg/L. Increasing fluoride concentration results in increasing Cr(VI) final concentrations. Fluoride ions showed an inhibitive effect towards the removal of Cr(VI) anions.

3.5. Electrocoagulation kinetics and adsorption isotherm

The principle of electrocoagulation modeling through adsorption isotherm and kinetics is based on the fact that the pollutant is generally adsorbed at the surface of the flocs anodically produced. Since the amount of coagulant can be

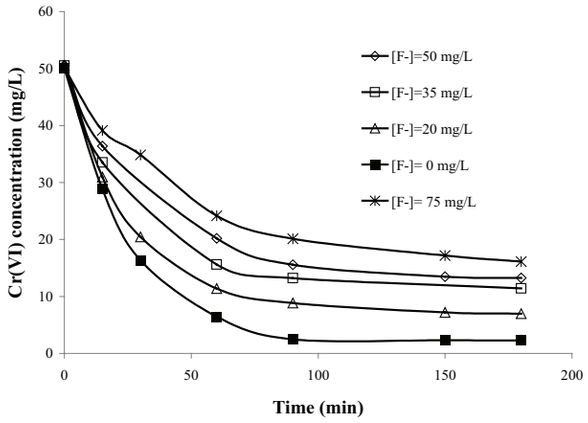

Fig. 9. Effect of fluoride concentration on Cr(VI) removal, pH_0, 3; current intensity 400 mA, $[Cr(VI)]_0$, 50 mg/L.

estimated for a given time, the pollutant removal can be modeled by adsorption phenomenon [20–23].

It has been proposed [20–23] that the general mechanism follows two consecutive separate steps:

(i) An electrochemical process through which the metal flocs are generated;
(ii) Adsorption of pollutants on the surface of the flocs.

Generally, the removal of pollutant with EC process is identical to conventional adsorption except the source of adsorbent. The mass of the later may be stoichiometrically deduced after calculating the mass of the dissolved metal according to Faraday's Law.

$$m = \frac{ItM}{nF} \tag{4}$$

where I is the applied current intensity (A), t is the electrolysis time (s), M is the molar mass of the anodic metal (g/mole), n is the number of implied electrons and F is the Faraday constant (96 485.3 coulomb/mole).

Consequently, pollutant removal can be modeled by adsorption phenomena [22,23] and the amount of adsorbed pollutant is:

$$q_t = \frac{V\left(C_0 - C_t\right)}{m} \tag{5}$$

where q_t is the adsorbed amount of pollutant per gram of adsorbent (mg/g), V is the volume of solution (L), m is the mass of the dissolved electrode (g); C_0 and C_t are the initial concentration and the concentration of pollutant at time t (mg/L), respectively. In order to investigate the mechanisms of the pollutant adsorption process, two main kinetic models were applied: pseudo-first-order, pseudo-second-order, to describe the adsorption kinetics onto metal hydroxides. The most accurate model was selected according to the linear regression correlation coefficient values, R^2.

The pseudo-first order kinetic model can be given as

$$\frac{dq}{dt} = K_1\left(q_e - q_t\right) \tag{6}$$

where K_1 (min^{-1}) is the constant rate of adsorption, q_t and q_e are the adsorbed amounts at a given time t and at equilibrium (mg/g) respectively. Integration Eq. (6) with boundary conditions $t = 0$ to t and $q_t = 0$ to q_t and rearrangement results in:

$$\ln\left(\frac{q_e - q_t}{q_e}\right) = -K_1 t \tag{7}$$

This may be rearranged to give:

$$\ln\ln\left(q_e - q_t\right) = \ln q_e - K_1 t \tag{8}$$

The slope of plot of log $(q_e - q_t)$ versus t was used to determine the pseudo-first-order rate constant K_1 [24]. The pseudo second-order model kinetic equation is:

$$\frac{dq}{dt} = K_2\left(q_e - q_t\right)^2 \tag{9}$$

where K_2 is the rate constant of the pseudo-second order equation (g/mg/min). Integration leads to:

$$\frac{t}{q_t} = \frac{1}{K_2 q_e^2} + \frac{t}{q_e} \tag{10}$$

Furthermore, adsorption isotherm models can be extended to describe EC experimental isotherm data and identify the mechanism of the adsorption process. Isotherm models with two and three parameters have been therefore considered to establish the relationship between the amounts of pollutant adsorbed onto the metal hydroxides and its equilibrium concentration in the aqueous solution containing pollutant. The general forms of both these models were described as follows.

The Langmuir equation:

$$\frac{C_e}{q_e} = \frac{1}{b} + \frac{q_0}{b} C_e \tag{11}$$

where b (L/mg) is the binding constant and q_0 (mg/g) refers the maximum adsorption capacity, evaluated by plotting the C_e/q_e against C_e.

The Freundlich isotherm:

$$\ln q_e = \ln K_f + \frac{1}{n} C_e \tag{12}$$

where K_f and n are the constants which give adsorption capacity and intensity respectively.

3.5.1. Kinetics modeling

Adsorption kinetics for fluoride and chromium was analyzed by first- and second-order using different initial concentrations. The adsorption kinetics (Tables 1–4) showed that the first order rate expression fitted well the adsorption kinetics for both pollutants. Similar trend was found by Vasudevan et al. [16] when studying hexavalent chromium removal by electrochemical coagulation using aluminium anodes. Mameri et al. [29] and Emamjomeh and Sivakumar [30] reported that the defluoridation rate of the EC-Al follows first order.

Table 1
First order kinetic model of different initial fluoride concentrations, pH_0, 3; current intensity 400 mA

Initial concentration fluoride (mg/L)	Q_{max} (mg g^{-1})	K_1 (min^{-1})	R^2
25	61.055	0.0541	0.998
35	85.038	0.0443	0.998
50	115.153	0.0474	0.999
75	174.421	0.02877	0.998
100	221.403	0.02621	0.992
150	309.26	0.0319	0.999

Table 2
First order kinetic model of different initial Cr(VI) concentrations, pH_0, 3; current intensity 400 mA

Initial concentration Cr(VI) (mg/L)	Q_{max} (mg g^{-1})	K_1 (min^{-1})	R^2
20	49.133	0.0395	0.995
35	83.29	0.0475	0.998
50	118.515	0.0368	0.998
75	165.458	0.0277	0.999
100	199.431	0.0175	0.998
150	254.423	0.029	0.991

Table 3
Second order kinetic model of different initial fluoride concentrations, pH_0, 3; current intensity 400 mA

Initial concentration fluoride (mg/L)	q_e (mg g^{-1})	K_2 (g mg^{-1} min^{-1})	R^2
25	67.925	$10.7.10^{-4}$	0.978
35	96.665	$5.955.10^{-4}$	0.953
50	125.632	$6.702.10^{-4}$	0.962
75	206.07	$1.711.10^{-4}$	0.968
100	268.42	$1.09.10^{-4}$	0.916
150	361.067	$1.134.10^{-4}$	0.950

Table 4
Second order kinetic model of different initial Cr(VI) concentrations, pH_0, 3; current intensity 400 mA

Initial concentration Cr(VI) (mg/L)	q_e (mg g^{-1})	K_2 (g mg^{-1} min^{-1})	R^2
20	56.953	$8.421.10^{-4}$	0.9687
35	93.774	$6.867.10^{-4}$	0.987
50	137.925	$3.243.10^{-4}$	0.987
75	187.305	$2.367.10^{-4}$	0.915
100	265.789	$0.5805.10^{-4}$	0.989
150	306.611	$0.1056.10^{-4}$	0.994

3.5.2. Adsorption isotherm

In order to describe the electrocoagulation process, the equilibrium adsorption behavior for fluoride and hexavalent chromium isanalyzed by fitting models of Langmuir and Freundlich isotherms at different initial concentrations. The results are depicted in Table 5. For both anions, the Freundlich adsorption isotherm resulted in the best fitting of the experimental equilibrium data. According to Bennajah et al. [31], the defluoridation reaction obeys the Freundlich law.

3.5.3. Effect of temperature and energy calculations

Figs. 10 and 11 show that the rate constants vary with temperature according to Eq. (13).

In our study, thermodynamic parameters, for example, enthalpy (ΔH), entropy (ΔS) and free energy (ΔG) of activation, were determined by using the following equations:

$$\log \frac{q_t}{C_t} = \frac{\Delta S^\circ}{2.303R} = \frac{\Delta H^\circ}{2.303R}\left(\frac{1}{T}\right) \quad (13)$$

where R = 8.314 J mol^{-1} K^{-1} is the ideal gas constant and T(K) the temperature in Kelvin.

$$\Delta G^\circ = \Delta H^\circ - \Delta S^\circ \quad (14)$$

The values of ΔH^0 and ΔS^0 were estimated from the slopes and intercepts of log q_t/C_t vs. 1/T.

Table 5
Constant parameters and correlation coefficients calculated for isotherm adsorption models of fluoride and Cr(VI)

	Langmuir			Freundlich		
	K_L	q_{max} (mg g^{-1})	R^2	K_F	n	R^2
Cr(VI)	0.431	234.413	0.903	80.548	0.298	0.964
Fuoride	0.189	341.775	0.889	83.463	0.391	0.981

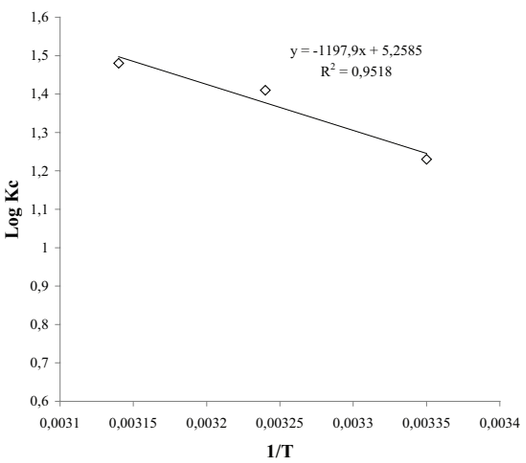

Fig. 10. Plot of Log K_c and 1/T, pH_0, 3; current intensity 400 mA; $[F^-]_0$, 100 mg/L.

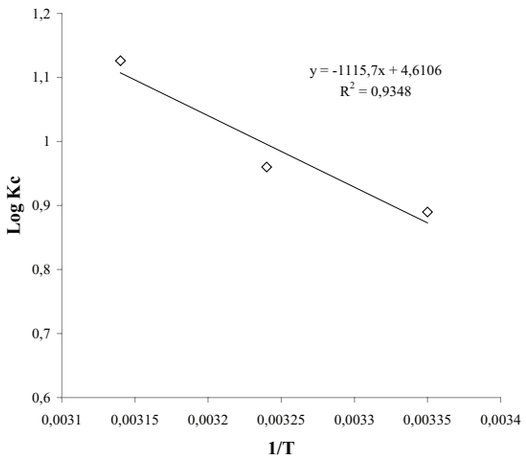

Fig. 11. Plot of Log K_c and 1/T, pH_0, 3; current intensity 400 mA, $[Cr(VI)]_0$, 100 mg/L.

Table 6
Thermodynamic parameters or adsorption of fluoride and Cr(VI)

	Fluoride	Cr(VI)
ΔH^0 (kJ·mol^{-1})	–22.919	–21.349
ΔS^0 (J·mol^{-1})	100,522	88.268
ΔG^0 (kJ·mol^{-1})		
298 K	–52.719	–47.650
308 K	–53.719	–48.533
318 K	–53.719	–49.415

The obtained results, given in the Table 6, showed clearly that the Gibbs free energy change (ΔG) is negative as expected for a spontaneous process under the applied conditions. The negative values of ΔG increase with temperature indicating more efficient sorption at high temperature.

The positive values of entropy change (ΔS) imply some structural change during the adsorption process of fluoride and Cr(VI) species onto aluminium hydroxides and the negative values of ΔH confirms the endothermic nature of the adsorption process. Identical results were found by Vasudevan et al. [32,33]. According to them, the improvement of adsorption capacity of aluminum hydroxide, by increasing temperature, may be attributed to the enlargement of pore size and/or activation of the adsorbent surface [22,34,35].

3.6. FT-IR Characterization of sludge before and after the adsorption of fluoride and Cr(VI)

FT-IR results revealed significant changes after pollutants adsorption and showed formation of new species on coagulants surface. Fig. 12 shows FT-IR spectra of aluminium sludge in absence (blue line) and presence (red line) of fluoride and Cr(VI) anions. The disappearance of the Al–OH band near 1130 cm^{-1} is due to fluoride adsorption. It was inferred that hydroxyl group Al–OH with bending vibration at 1129 cm^{-1} had reacted with fluoride ions [36]. In addition, disappearance of peak 1526 cm^{-1} was also

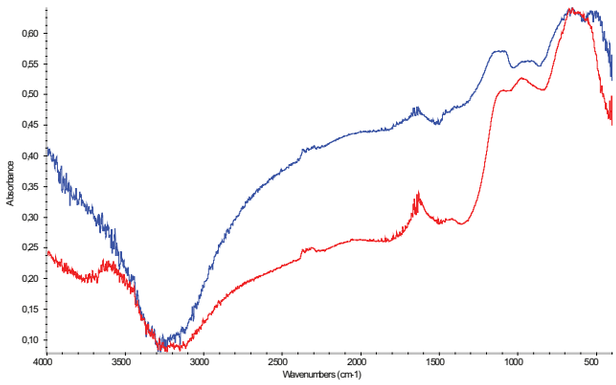

Fig. 12. FT-IR spectra, in absence (blue line) and in presence of fluoride and Cr(VI) ions (red line).

observed [37]. This peak corresponded to stretching and bending modes of Al–O. After adsorbing fluoride anions, this band disappeared. This may be ascribed to substitution of hydroxyl groups on $Al(OH)_3$ precipitates by fluoride ions [38]. The appearance of the peak at 897 cm^{-1}, which is characteristic of chromate (CrO_4^{2-}), indicates that Cr(VI) species adsorption on coagulant takes place. Furthermore, disappearance of band at 545 cm^{-1} indicates stretching and bending modes of Al–O are affected by fluoride adsorption [39].

4. Conclusion

The removal of fluoride and Cr(VI) ions from photovoltaic wastewater by EC was successfully achieved in single and binary systems. The results showed that the removal of both pollutants from synthetic wastewater was strongly affected by initial pH, current intensity and initial concentration. The optimal initial pH was found at pH 3. Increasing current intensity results in improving removal efficiency for both pollutants. Increasing initial concentration was found detrimental for removal efficiency. The study of the simultaneous removal reveals negative effect of presence of one pollutant towards the other, suggesting antagonistic adsorption competition on electrochemically produced coagulants. First order and second order adsorption kinetic models were examined to model single adsorption. First order model gives the best fitting. The mechanism of the single electrocoagulation was modeled using Langmuir and Freundlich isotherm models and the latter matched preferably experimental data. For binary system, obtained results showed that the removal of one pollutant is inhibited by the presence of the other. The simultaneous removal study reveals existence of competition between the two pollutants with an antagonist effect. Thermodynamic parameters, including the Gibbs free energy, enthalpy, and entropy, indicated that the adsorption of the two pollutants on aluminium hydroxides was feasible, spontaneous and endothermic.

Acknowledgements

Authors would like to thank the DGRSDT/MESRS Algeria for financially supporting this research.

References

[1] M.D.G. de Luna, Warmadewanthi, J.C. Liu, Combined treatment of polishing wastewater and fluoride-containing wastewater from a semiconductor manufacturer, Colloids Surf. A Physicochem. Eng. Asp., 347 (2009) 64–68.

[2] N. Drouiche, S. Aoudj, M. Hecini, T. Ouslimane, Experimental design for the elimination of fluoride from pretreated photovoltaic wastewater by electrocoagulation, Chem. Eng. Trans., 24 (2011) 1207–1212.

[3] F. Seccod'Aragona, Dislocation etch for (100) planes in silicon, J. Electrochem. Soc., 119 (1972) 948–951.

[4] K.H. Yang, An etch for delineation of defects in silicon, Electrochem. Soc., 131 (1984) 1140–1145.

[5] M. Fathi, A. Chikouche, New method for quality evaluation of Mc-Si wafers implied in the fabrication of photovoltaic cells, Jordan J. Mech. Indust. Eng., 4 (2010) 151–154.

[6] S. Aoudj, A. Khelifa, N. Drouiche, R. Belkada, D. Miroud, Simultaneous removal of chromium(VI) and fluoride by electrocoagulation–electroflotation: Application of a hybrid Fe-Al anode, Chem. Eng. J., 267 (2015) 153–162.

[7] C.Y. Hu, S.L. Lo, W.H. Kuan, Y.D. Lee, Removal of fluoride from semiconductor wastewater by electrocoagulation–flotation, Water Res., 39 (2005) 895–901.

[8] G. Sozhan, S. Mohan, S. Vasudevan , R Balaji, S. Pushpavanam, Recovery of chromium from the solid residue by in-situ-generated hypochlorite, Ind. Eng. Chem. Res., 45 (2006) 7743–7747.

[9] M. Rajiv Gandhi, S. Vasudevan, A. Shibayama, M. Yamada, Graphene and graphene-based composites: a rising star in water purification - a comprehensive overview, Chem. Select, 15 (2016) 4357–5073.

[10] S. Vasudevan, M.A. Oturan, Electrochemistry as cause and cure in water pollution. An overview, Environ. Chem. Lett., 12 (2014) 97–108.

[11] A. Khelifa, S. Aoudj, S. Moulay, M. Hecini, M. de Petris-Wery, Degradation of EDTA by in-situ electrogenerated active chlorine in an electroflotationcell, Desal. Water Treat., 7 (2009) 119–123.

[12] G. Chen, Electrochemical technologies in wastewater treatment, Sep. Purif. Technol., 38 (2004) 11–41.

[13] S. Vasudevan, G. Sozhan, S. Mohan, R. Balaji, P. Malathy, S. Pushpavanam, Electrochemical regeneration of chromium containing solution from metal finishing industry, Ind. Eng. Chem. Res., 46 (2007) 2898–2901.

[14] S. Aoudj, A. Khelifa, N. Drouiche, M. Hecini, HF wastewater remediation by electrocoagulation process, Desal. Water Treat., 51 (2013) 1596–1602.

[15] C. Barrera-Diaz, V. Lugo-Lugo, G. Roa-Morales, R. Natividad, S.A. Martinez-Delgadillo, Enhancing the electrochemical Cr(VI) reduction in aqueous solution, J. Hazard. Mater., 185 (2011) 1362–1368.

[16] S. Vasudevan, J. Lakshmi, R. Vanathi, Electrochemical coagulation for chromium removal: process optimization, kinetics, isotherms and sludge characterization, CLEAN–Soil, Air, Water, 38 (2010) 9–16.

[17] S. Vasudevan, J. Lakshmi, G. Sozhan, Studies on the Al–Zn–In-alloy as anode material for the removal of chromium fromdrinking water in electrocoagulation process, Desalination, 275 (2011) 260–268.

[18] R. Kamaraj, P. Ganesan, S. Vasudevan, Removal of lead from aqueous solutions by electrocoagulation: isotherm, kinetics and thermodynamic studies, Int. J. Environ. Sci. Technol., 12 (2015) 683–692.

[19] N. Balasubramanian, Toshinori Kojima, C. Srinivasakannan, Arsenic removal through electrocoagulation: Kinetic and statistical modelling, Chem. Eng. J., 155 (2009) 76–82.

[20] K.N. Chithra, N. Balasubramanian, Modeling electrocoagulation through adsorption kinetics, J. Model. Simulat. Syst., 1 (2010) 124–130.

[21] Y. AitOuaissa, M. Chabani, A. Amrane, A. Bensmaili, Removal of tetracycline by electrocoagulation: Kinetic and isotherm modeling through adsorption, J. Environ. Chem. Eng., 2 (2014) 177–184.

[22] S. Vasudevan, B.S. Kannan, J. Lakshmi, S. Mohanraj, G. Sozhan, Effects of alternating and direct current in electrocoagulation process on the removal of fluoride from water, J. Chem. Technol. Biotech., 86 (2011) 428–436.

[23] S. Vasudevan, J. Lakshmi, G. Sozhan, Studies on a Mg-Al-Zn Alloy as an anode for the removal of fluoride from drinking water in an electrocoagulation process, CLEAN–Soil, Air, Water, 37 (2009) 372–378.

[24] F. Zermane, B. Cheknane, J. Ph. Basly, O. Bouras, M. Baudu, Influence of humic acids on the adsorption of Basic Yellow 28 dye onto an iron organo–inorgano pillared clay and two hydrous ferric oxides, J. Colloid. Inter. Sci., 395 (2013) 212–216.

[25] APHA, Standard Methods for the Examination of Water and Wastewater, 17th ed., American Public Health Association, Washington D.C., 1992.

[26] S. Sadeghi, M.R.A Moghaddam, M. Arami, Improvement of electrocoagulation process on hexavalent chromium removal with the use of polyaluminum chloride as coagulant, Desal. Water Treat., 52 (2014) 4818–4829.

[27] G. Mouedhen, M. Feki, M. De Petris-Wery, H.F. Ayedi, Electrochemical removal of Cr(VI) from aqueous media using iron and aluminum as electrode materials: Towards a better understanding of the involved phenomena, J. Hazard. Mater., 168 (2009) 983–991.

[28] M.G. Kılıç, Ç. Hoşten, Ş. Demirci, A parametric comparative study of electrocoagulation and coagulation using ultrafine quartz suspensions, J. Hazard. Mater., 171 (2009) 247–252.

[29] N. Mameri, A.R. Yeddou, H. Lounici, D. Belhocine, H. Grib, B. Bariou, Defluoridation of septentrional Sahara water of north Africa by electrocoagulation process using bipolar aluminium electrodes, Water Res., 32 (1998) 1604–1612.

[30] M.M. Emamjomeh, M. Sivakumar, An empirical model for defluoridation by batch monopolarelectrocoagulation/flotation (ECF) process, J. Hazard. Mater., 131 (2006) 118–125.

[31] M. Bennajah, Y. Darmane, M. EbnTouhami, M. Maalmi, A variable order kinetic model to predict defluoridation of drinking water by electrocoagulation-electroflotation, Int. J. Eng. Sci. Technol., 2 (2010) 42–52.

[32] S. Vasudevan, J. Lakshmi, Studies relating to an electrochemically assisted coagulation for the removal of chromium from water using zinc anode, Water Sci. Technol.: Water Supply, 11 (2011) 142–150.

[33] S. Vasudevan, J. Lakshmi, G. Sozhan, Simultaneous removal of Co, Cu, and Cr from water by electrocoagulation, Toxicol. Environ. Chem., 94 (2012) 1930–1940.

[34] R. Kamaraj, A. Pandiarajan, S. Jayakiruba, M. Naushad, S. Vasudevan, Kinetics, thermodynamics and isotherm modeling for removal of nitrate from liquids by facile one-pot electrosynthesized nano zinc hydroxide, J. Mol. Liq., 215 (2016) 204–211.

[35] R. Kamaraj, S. Vasudevan, Facile one-pot synthesis of nano-zinc hydroxide by electro-dissolution of zinc as a sacrificial anode and the application for adsorption of Th^{4+}, U^{4+}, and Ce^{4+} from aqueous solution, Res. Chem. Intermed., 42 (2016) 4077–4095.

[36] L. Chen, H.X. Wu, T.J. Wang, Y. Jin, Y. Zhang, X.M. Dou, Granulation of Fe–Al–Ce nano-adsorbent for fluoride removal from drinking water by spray coating on sand in a fluidized bed, Powder Technol., 193 (2009) 59–64.

[37] R. Liu, W. Gong, H. Lan, T. Yang, H. Liu, J. Qu, Simultaneous removal of arsenate and fluoride by iron and alum binary oxide: competitive adsorption effects, Sep. Purif. Technol., 92 (2012) 100–105.

[38] R. Liu, W. Gong, H. Lan, Y. Gao, H. Liu, J. Qu, Defluoridation by freshly prepared Aluminum hydroxides, Chem. Eng. J., 175 (2011) 144–149.

[39] M. Gude Sujana, S. Anand, Iron and aluminium based mixed: a novel sorbent for fluoride removal from aqueous solutions, Appl. Surf. Sci., 256 (2010) 6956–6962.

[40] N. Drouiche, S. Aoudj, M. Hecini, N. Ghaffour, H. Lounici, N. Mameri, Study on the treatment of photovoltaic wastewater using electrocoagulation: Fluoride removal with aluminium electrodes—Characteristics of products. J. Hazard. Mater., 169(1–3) (2009) 65–69.

[41] N. Drouiche, N. Ghaffour, H. Lounici, N. Mameri, A. Maallemi, H. Mahmoudi, Electrochemical treatment of chemical mechanical polishing wastewater: removal of fluoride — sludge characteristics — operating cost, Desalination, 223(1–3) (2008) 134–142.
[42] N. Drouiche, S. Aoudj, H. Lounici, H. Mahmoudi, N. Ghaffour, M.F.A. Goosen, Development of an empirical model for fluoride removal from photovoltaic wastewater by a bipolar electrocoagulation process, Desal. Water Treat., 29 (2011) 96–102.
[43] B. Palahouane, N. Drouiche, S. Aoudj, K. Bensadok, Cost effective electrocoagulation process for the remediation of Fluoride from pretreated photovoltaic wastewater, J. Ind. Engng. Chem., 2 (2015) 127–131.
[44] K. Cheballah, A. Sahmoune, K. Messaoudi, N. Drouiche, H. Lounici, Simultaneous removal of hexavalent chromium and COD from industrial wastewater by bipolar electrocoagulation, Chem. Engng. Process.: Process Intensification, (2015) 94–99.